

Substituent effects on cellulose dissolution in imidazolium-based ionic liquids

Niwanthi Dissanayake · Vidura D. Thalangamaarachchige · Shelby Troxell · Edward L. Quitevis  · Nouredine Abidi 

Received: 23 April 2018 / Accepted: 28 September 2018 / Published online: 24 October 2018
© Springer Nature B.V. 2018

Abstract The dissolution of cotton cellulose with ionic liquids (ILs) has been extensively studied. However, the mechanism of cellulose dissolution, especially the role of the IL cation in the dissolution process, is not well understood. This paper describes a systematic study of the effects of the substituent groups on the cation in imidazolium-based ILs on cellulose dissolution. A series of imidazolium-based ILs with acetate as the anion, 1-heptyl-3-methylimidazolium acetate ([C₇C₁im][OAc]), 1-(cyclohexylmethyl)-3-methylimidazolium acetate ([CyhmC₁im][OAc]), 1-benzyl-3-methylimidazolium acetate ([BnzC₁im]

[OAc]), 1,3-dibenzylimidazolium acetate ([Bnz)₂im][OAc]), and 1-(2-naphthylmethyl)-3-methylimidazolium acetate ([NapmC₁im][OAc]) were synthesized. In each dissolution experiment, 5% (w/w) ground cotton fiber was dissolved in the ILs at 90 °C. The progress of the dissolution was monitored periodically with a polarized light microscope. This study revealed that [BnzC₁im][OAc] dissolved cotton cellulose more efficiently than the other four ILs. The results are discussed within the context of previous published theoretical and experimental studies on cellulose dissolution in ILs. For the five ILs that were investigated, we find that the effect of the cation can be rationalized on the basis of both the size and shape of the cation. In addition to the dissolution, cellulose was regenerated and characterized by Fourier transform infrared (FTIR) spectroscopy and scanning electron microscopy (SEM).

Electronic supplementary material The online version of this article (<https://doi.org/10.1007/s10570-018-2055-1>) contains supplementary material, which is available to authorized users.

Niwanthi Dissanayake and Vidura D. Thalangamaarachchige have contributed equally to this work.

N. Dissanayake · N. Abidi (✉)
Fiber and Biopolymer Research Institute, Department of Plant and Soil Science, Texas Tech University, Lubbock, TX 79403, USA
e-mail: noureddine.abidi@ttu.edu

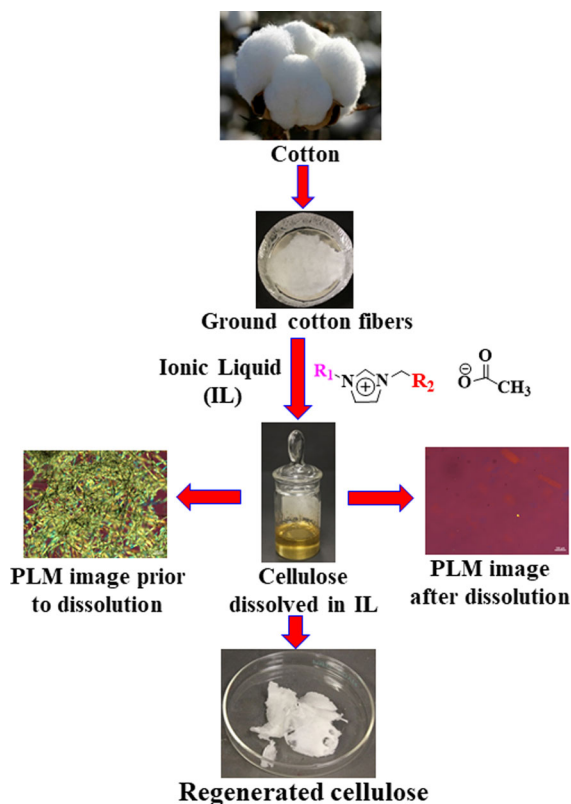
N. Dissanayake
e-mail: niwanthi.dissanayake@ttu.edu

V. D. Thalangamaarachchige · S. Troxell · E. L. Quitevis (✉)
Department of Chemistry & Biochemistry, Texas Tech University, Lubbock, TX 79409, USA
e-mail: edward.quitevis@ttu.edu

V. D. Thalangamaarachchige
e-mail: vidura.d.thalangamaarachchige@ttu.edu

S. Troxell
e-mail: shelby.troxell@ttu.edu

Graphical abstract



Keywords Cellulose · Ionic liquids · Fourier transform infrared spectroscopy · Polarized light microscopy

Introduction

Cellulose is the most abundant, natural, renewable, and biodegradable polymer on earth. Cellulose can be obtained from various sources, such as rice, wheat, sugar cane, and other agricultural products, as well as from bacteria (Azizi Samir et al. 2005; Heinze et al. 2008). Cotton is the most cellulose-rich plant species. Mature cotton fiber contains > 90% crystalline cellulose, including its cellulosic secondary wall, which is surrounded by the cuticulated primary wall (Haigler et al. 2012). The cellulose in cotton fiber has numerous applications. However, many of these applications require the cotton to be dissolved first (Ragauskas et al. 2006; Gericke et al. 2012). The crystalline

structure and the strong hydrogen-bond network make it thermally and chemically stable. As a result, cellulose is difficult to dissolve in water or common organic solvents.

In recent years, ionic liquids (ILs) have been proposed as solvents for biopolymers (Madeira Lau et al. 2004; Phillips et al. 2004). Compared to conventional organic solvents, ILs have unique features such as negligible vapor pressure, non-flammability, high chemical and thermal stability, and the ability to dissolve many organic and inorganic materials (Welton 1999; Rogers and Seddon 2003; Pinkert et al. 2009; Sun et al. 2011). Rogers and Seddon (2003) showed that imidazolium-based ILs with strong hydrogen-bonding anions are able to dissolve cellulose upon heating. In case of the IL, 1-butyl-3-methylimidazolium chloride ($[C_4C_1im][Cl]$), the rate of cellulose dissolution was greatly improved when heated in a microwave oven with pulsing at full power (Swatloski et al. 2002). Recent studies also found that some ILs can dissolve cellulose at lower temperatures and that the ILs can be easily recovered by a recycling process (Zhang et al. 2005; Kosan et al. 2008; Vitz et al. 2009; Abe et al. 2010; Xu et al. 2010; Lan et al. 2011). One of the advantages of using ILs to dissolve cellulose is the ability to tune the chemical and physical properties of ILs by varying the structures of cations and anions (Zhang et al. 2006). This allows one to systematically study the mechanism of cellulose dissolution.

It is generally accepted that the interaction of anions of ILs with the hydroxyl groups of cellulose to form hydrogen bonds plays a key role in the dissolution of cellulose. However, the mechanism of cellulose dissolution is still not well understood (Yao et al. 2015). In particular, despite the various studies to date on the dissolution of cellulose by ILs, there are conflicting explanations for the role of the cation in the dissolution of cellulose (Xu et al. 2012; Lu et al. 2014). For example, the mechanism of carbohydrate dissolution in acetate and chloride containing ILs was examined by utilizing ^{13}C and $^{35/37}Cl$ relaxation rates of the corresponding anions (Remsing et al. 2006, 2008). These studies indicate that the relaxation time depends strongly on the cellulose content, but only slight variations of the relaxation time were observed when the cation was varied. These results suggest that the cation plays a minor role in the cellulose dissolution. Youngs et al. utilized 1H NMR

and molecular dynamics (MD) simulations to study the interactions between glucose and ILs, such as 1-ethyl-3-methylimidazolium acetate ($[\text{C}_2\text{C}_1\text{im}][\text{OAc}]$) and 1,3-dimethylimidazolium chloride ($[\text{C}_1\text{C}_1\text{im}][\text{Cl}]$) (Youngs et al. 2007, 2011). They found that the major interaction was between the anion of the IL and the hydrogens of the hydroxyl groups on the glucose units, whereas there were only minor interactions between the cation and the glucose units (Youngs et al. 2006). In contrast, a study of the interaction of 1-butyl-3-methylimidazolium acetate ($[\text{C}_4\text{C}_1\text{im}][\text{OAc}]$) with cellobiose by Zhang et al. revealed that both the cation and anion were required in the dissolution process (Zhang et al. 2005). A study by Lindman et al. reported that the hydrophobic interactions between the cations of ILs and cellulose are the main driving forces in dissolution (Lindman et al. 2010). Another study by Olsson and Westman confirmed that the anion of the IL penetrates the cellulose and disassembles the cellulose structure by competitive hydrogen bonding (Olsson and Westman 2013). Lu et al. proposed that the cation plays a more prominent role than had been previously thought. They hypothesized that the cation and anion should be sufficiently small enough to reach the hydroxyl groups of cellulose (Lu et al. 2014). They further proposed that electron donor-acceptors also play a role in cellulose dissolution by breaking up cellulose–cellulose hydrogen bonding interactions. The computational studies performed by Gupta and Jiang indicated that the dissolution of cellulose in ILs is initiated by the disruption of hydrogen bonds in cellulose (Gupta and Jiang 2015). This was mainly through the formation of hydrogen bonds between the anions and cellulose and the hydrophobic interactions with the cations.

Several MD simulation studies were performed by Mostofian et al. to understand the interactions between ILs and cellulose. In one of their earlier simulations, they studied the solute–solvent interactions at the interface of a cellulose microfibril in $[\text{C}_4\text{C}_1\text{im}][\text{Cl}]$ (Mostofian et al. 2011). In their recent study, the authors investigated the structure and dynamics of cellulose decramer in both water and $[\text{C}_4\text{C}_1\text{im}][\text{Cl}]$. In this study, they focused on the interactions of the anion and the cation of $[\text{C}_4\text{C}_1\text{im}][\text{Cl}]$ with glucan chains. They observed ring-stacking interactions between the cations and the hydrophobic surface of cellulose (Mostofian et al. 2014). Several studies have been reported in which the conductor like screening model for real

solvents (COSMO-RS) was used to screen ILs and to study the interactions between ILs and cellulose models (Kahlen et al. 2010; Casas et al. 2012, 2013; Liu et al. 2016). Kahlen et al. studied the interactions between trisaccharide and ILs (Kahlen et al. 2010). Casas et al. used the excess enthalpy of mixing as a reference property in COSMO-RS to study the solubility of cellulose in ILs and found that the main force involves hydrogen bonding (Casas et al. 2012). They optimized a 3×3 cellulose model for use in COSMO-RS calculations to predict the ability of ILs to dissolve cellulose (Casas et al. 2013). Lu et al. found that the mid-monomer part of cellotriose was the model to use in COSMO-RS calculations for predicting the solubility of cellulose in ILs (Liu et al. 2016).

Although most studies to date show that the anions play an important role in the dissolution of cellulose in ILs, there is still not a clear understanding of the role of the cation and the mechanism of dissolution. Recent molecular dynamics (MD) simulations by Rabideau et al. and Li et al. provided molecular-level insights into the interactions of ionic species in ILs with cellulose and the possible mechanism for cellulose dissolution in ILs (Rabideau et al. 2014; Li et al. 2015). Rabideau et al. performed a systematic MD simulation study of the dissolution of cellulose in three ILs: $[\text{C}_2\text{C}_1\text{im}][\text{OAc}]$, $[\text{C}_4\text{C}_1\text{im}][\text{Cl}]$, and $[\text{C}_1\text{C}_1\text{im}][\text{DMP}]$, where $[\text{DMP}]^-$ is the dimethyl phosphate anion. In their study, the breakup of small bundles of cellulose I_α and I_β in the ILs $[\text{C}_4\text{C}_1\text{im}][\text{Cl}]$, $[\text{C}_2\text{C}_1\text{im}][\text{OAc}]$, and $[\text{C}_1\text{C}_1\text{im}][\text{DMP}]$ were investigated. According to their results, anions first bind strongly to the hydroxyl groups of the exterior strands of the bundle, forming negatively charged complexes. The binding of anions to hydroxyl groups deteriorates the intrastrand hydrogen bonds present in the cellulose strands, reducing the rigidity of the strands. Then, due to charge imbalances, the cations intercalate between strands. This provides the bulk to push the individual strands apart and to initiate separation. Rabideau et al. observed the peeling of an individual strand from the main bundle in $[\text{C}_2\text{C}_1\text{im}][\text{OAc}]$. This led to disruption of the hydrogen bonds with other strands, resulting in chain detachment of the individual glucan units from the main bundle.

Li et al. performed long (3 ms) MD simulations on a cellulose bundle comprised of 4 strands, each with 8 glucose units, and a cellulose bundle comprised of 7 strands, each with 8 glucose units, in $[\text{C}_2\text{C}_1\text{im}][\text{OAc}]$,

[C₂C₁im][Cl] and [C₄C₁im][Cl]. The behavior of the cellulose bundles in these ILs is similar to that observed by Rabideau et al. In their MD simulations Li et al. observed complete breakup of the 7-strand bundle in 500 ns for [C₂C₁im][OAc], but observed little change for [C₂C₁im][Cl] and [C₄C₁im][Cl] in the same time period. They observed that for [C₂C₁im][OAc], the [OAc][−] ions bind tightly to the hydroxyl groups, thus weakening the binding between the neighboring cellulose sheets due to [OAc][−] larger size compared to that of [Cl][−]. This allows more ions to enter into the cellulose gap. However, in contrast to MD simulations of Rabideau et al., those of Li et al. showed the cations having strong van der Waals interactions with cellulose.

In this work, we investigated the effect of different substituents on the imidazolium ring of the cation of the ILs in cellulose dissolution. In our study, five ILs consisting of a fixed acetate [OAc][−] anion and a 1-R-3-methylimidazolium cation functionalized by various R groups with R = n-heptyl (C₇), cyclohexylmethyl (Cyhm), 2-naphthylmethyl (Napm), and benzyl (Bnz) were synthesized, as well the dibenzyl cation [(Bnz)₂im]⁺ and were used in cotton cellulose dissolution (see Table 1).

The aforementioned ILs allowed us to study the effect of the substituents on the N atoms of the imidazolium cations. In particular, we were able to

study how the dissolution is affected by having cyclic alkyl, linear alkyl chain and planar aromatic substituents. The trends observed in these five ILs are discussed within the context of the theoretical and experimental results reported in the literature. According to the study performed by Liu et al. the interactions between aromatic substituent groups, such as benzyl, and cellulose occur mainly through van der Waals forces and CH-π interactions. The alkyl chains and cyclic alkyl group interact with cellulose via van der Waals forces while the cations as a whole interact through hydrophobic interactions with cellulose. The acetate anions predominantly interact with cellulose through hydrogen bonding (Liu et al. 2010).

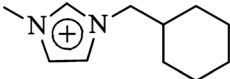
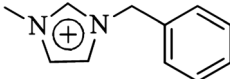
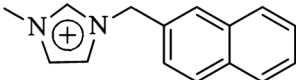
Experimental section

Materials and methods

Materials

1-Methylimidazole (Sigma, 98.9%), 2-(bromomethyl)naphthalene (Sigma, 96%), (bromomethyl)cyclohexane (Sigma, 99%), benzyl bromide (Sigma, 98%) 1-bromoheptane (Sigma, 99%), 1-methylimidazole (Sigma, 99%), Amberlite IRA-400 chloride resin (Sigma) were used without

Table 1 Structures and formulas of imidazolium-based cations

Cation	Cation structure	vdW Volume ^a (Å ³)	Abbreviation	Formula
1-heptyl-3-methylimidazolium		261.3	[C ₇ C ₁ im] ⁺	C ₁₁ H ₂₁ N ₂ ⁺
1-(cyclohexylmethyl)-3-methylimidazolium		232.0	[CyhmC ₁ im] ⁺	C ₁₁ H ₁₉ N ₂ ⁺
1-benzyl-3-methylimidazolium		222.9	[BnzC ₁ im] ⁺	C ₁₁ H ₁₃ N ₂ ⁺
1,3-dibenzylimidazolium		303.6	[(Bnz) ₂ im] ⁺	C ₁₇ H ₁₇ N ₂ ⁺
1-(2-naphthylmethyl)-3-methylimidazolium		269.3	[NapmC ₁ im] ⁺	C ₁₅ H ₁₅ N ₂ ⁺

^aVan der Waals volume from AM1 quantum calculations using Spartan 10 (Wavefunction, Inc)

further purification. Dichloromethane (DCM) and acetonitrile were separately distilled over CaH₂ under nitrogen and diethyl ether was distilled over Na/benzophenone. A 1 N NaOH solution was prepared by dissolving 40 g of NaOH (Fisher) in 1 L of deionized water for anion exchange with chloride. For the gravitational column chromatography, Celite (Fisher), sand (Macros), aluminium oxide (60A, activated, basic, 50–200 micron, Acros) and glass wool were used. Acetic acid (Sigma) was used for neutralization. All the ILs were dried in a vacuum oven at 50 °C for 96 h. After drying, the water content was less than 400 ppm, as measured by Karl Fisher titration (Karl Fisher METTLER TOLEDO C20 coulometric KF titrator). Halides were undetectable as measured by AgNO₃ precipitation. Other impurities were undetectable as measured by NMR with a JEOL 400 MHz spectrometer. All the synthesized ILs have a purity of more than 98%, as determined by a reported protocol (Thakurathi et al. 2018). ¹H and ¹³C NMR spectra were recorded on a JEOL ECS 400 MHz spectrometer. For ¹H NMR spectra, tetramethylsilane (TMS, δ = 0.00) or the residual protic solvent peak (for (CD₃)₂CO, δ = 2.05, DMSO-d₆, δ = 2.50) and for ¹³C NMR spectra, tetramethylsilane (TMS, δ = 0.00) or the residual solvent peak (for (CD₃)₂CO, δ = 29.84, DMSO-d₆, δ = 39.50) served as shift references. Coupling constants, *J*, are reported in hertz. All reaction vessels were flame-dried under vacuum and filled with nitrogen prior to use. All reactions were performed under a nitrogen atmosphere as a routine practice, not as an essential requirement.

Synthesis of ionic liquids

The synthesis of the corresponding bromide ILs was performed via quaternization reactions. Stoichiometric amounts of 1-methylimidazole were reacted with benzyl bromide, (bromomethyl)cyclohexane, 2-(bromomethyl)naphthalene, 1-bromoheptane to yield 1-benzyl-3-methylimidazolium bromide ([BnzC₁im][Br]), 1-(cyclohexylmethyl)-3-methylimidazolium bromide ([CyhmC₁im][Br]), 1-(2-naphthylmethyl)-3-methylimidazolium bromide ([NapmC₁im][Br]) and 1-heptyl-3-methylimidazolium bromide ([C₇C₁im][Br]), respectively. 1,3-dibenzylimidazolium bromide [(Bnz)₂im][Br] was synthesized by reacting imidazole with 1 eq. of NaH in THF followed by the addition of 2 eq. of benzyl bromide. All these bromide ILs were

isolated, purified and characterized by NMR before the anion exchange reactions.

1-(2-methylcyclohexyl)-3-methylimidazolium acetate ([CyhmC₁im][OAc]) was prepared as follows. 1-(2-methylcyclohexyl)-3-methylimidazolium bromide ([CyhmC₁im][Br]) was dissolved in deionized water, and the resulting solution was passed through a column filled with anion exchange resin (Amberlite IRA-400) and flushed with 1 N NaOH to yield an aqueous solution of 1-(2-methylcyclohexyl)-3-methylimidazolium hydroxide ([CyhmC₁im][OH]). Acetic acid aqueous solution was added dropwise to the aqueous [CyhmC₁im][OH] solution and the resulting solution was stirred overnight at room temperature. After removal of water by evaporation, the residual liquid was repeatedly washed with excess amounts of anhydrous diethyl ether. The resulting liquid was fully mixed with DCM, followed by the addition of activated carbon and the mixture was stirred for 3 days. The mixture was passed through a gravitational column filled with active alumina, Celite and sand. DCM was removed by rotary evaporation and the resulting liquid was dried *in vacuo* at room temperature, yielding [CyhmC₁im][OAc] as a pale yellow liquid. [C₇C₁im][OAc], [BnzC₁im][OAc], [NapmC₁im][OAc] and [(Bnz)₂im][OAc] were prepared using similar procedures with the corresponding IL bromides (see Supplementary Information for details of the synthesis of the IL acetates and bromides.) The chemical structures of the synthesized ILs were confirmed by ¹H and ¹³C NMR spectra (see Supplementary Information).

Preparation of cotton fibers for dissolution

Carded cotton fibers were received from the Fiber and Biopolymer Research Institute, Texas Tech University. The fibers were scoured, bleached, air-dried, and ground by a Wiley mill to pass through a 20 mesh screen. They were dried at 105 °C overnight in a laboratory oven.

Dissolution of ground cotton fibers in ILs

[(Bnz)₂im][OAc] and [NapmC₁im][OAc] were heated at 85 °C in a laboratory oven until they became fluid enough to allow for stirring. The ILs and ground cotton fiber (5 wt%) were measured separately and the ground cotton fiber samples were slowly added to the

ILs. The dispersions were heated to 90–100 °C with several 3–5 s pulses in a regular household microwave oven (1500 W). The mixtures were placed in a 90 °C laboratory oven and continuously heated for 24 h.

Polarized light microscopy (PLM)

Representative samples of the solution were taken in 4 different time intervals (before and after the solutions were microwaved, and after 4 and 24 h at 90 °C). The mixtures were stirred prior to the samples being collected. The dissolution processes in the different ILs were observed by a Nikon ECLIPSE LV 100 polarizing light microscope with NIS-Elements imaging platform. The images were recorded at room temperature under X10 magnification.

Regeneration of cellulose from the mixtures

Each cotton-IL solution was poured onto a glass slide and covered with another glass slide. They were allowed to spread uniformly by gently pressing the glass slides. The glass slides that contained cotton-IL solutions were kept in a glass jar. Deionized water was poured on to the glass slides to regenerate cellulose from the solutions. The ILs were rinsed away from the regenerated cellulose by changing the deionized water for 3–4 days.

Freeze drying the regenerated cellulose

The regenerated cellulose from the different ILs were kept at – 4 °C for 2 h and dried using a Labconco FreeZone (4.5 Liter Cascade Benchtop Freeze Dry System) at – 102 °C and 0.05 mbar for 3 days.

Characterization of the regenerated cellulose

Scanning electron microscopy Scanning electron micrographs of the regenerated cellulose samples were recorded using a Hitachi TM-1000 tabletop environmental scanning electron microscope at an accelerating voltage of 15 kV. The regenerated cellulose samples were mounted on carbon discs without any coating prior to obtaining the images.

Fourier transform infrared spectroscopy (FTIR) The freeze-dried, regenerated cellulose

samples and hot dried ground cotton fibers were conditioned in the laboratory at 21 ± 1 °C at $65 \pm 2\%$ relative humidity for 2 days before the FTIR analysis. FTIR spectra of all regenerated samples were collected using a Perkin-Elmer Spectrum 400 FTIR spectrometer equipped with a universal attenuated total reflectance (UATR) accessory. The Zn-diamond crystal was cleaned with Milli-Q water and ethanol and a background scan of the clean crystal was performed prior to scanning the samples. The samples were placed on the Zn-diamond crystal without further sample preparation. Constant pressure was applied to each sample by the “pressure arm” of the instrument, which was monitored by the Perkin-Elmer software to minimize the loss of intensity of IR beam. The spectra were collected in the mid-IR range from 650 to 4000 cm^{-1} at a resolution of 4 cm^{-1} with 32 co-added scans. The spectra were subjected to baseline correction and normalization using the Perkin-Elmer software.

Results and discussion

Results

Polarized light microscopy of cellulose dissolution

Figure 1 shows PLM images of the 5% (w/w) mixtures for the five ILs at different stages of cellulose dissolution: before microwaving (Fig. 1a–e), after microwaving (Fig. 1f–j), after 4 h of heating at 90 °C (Fig. 1k–o); and after 24 h of heating at 90 °C (Fig. 1p–t). Because of the extensive crystalline structure of native cellulose, PLM is able to show the state of cellulose fiber-IL mixtures during dissolution. The PLM images of the mixtures before microwaving (Fig. 1a–e) provide a reference with which to compare the other stages of dissolution. As can be seen in the PLM images before microwaving (Fig. 1a–e) and after microwaving (Fig. 1f–j), the heating during microwaving causes dissolution to occur to varying extent depending upon the IL.

In the case of $[\text{C}_7\text{C}_1\text{im}][\text{OAc}]$, $[\text{CyhmC}_1\text{im}][\text{OAc}]$, $[(\text{Bnz})_2\text{im}][\text{OAc}]$, and $[\text{NapmC}_1\text{im}][\text{OAc}]$, relatively low dissolution occurred after microwaving. In contrast, there was noticeable cellulose dissolution in $[\text{BnzC}_1\text{im}][\text{OAc}]$ after microwaving, as evidenced by regions showing the absence of crystalline cellulose.

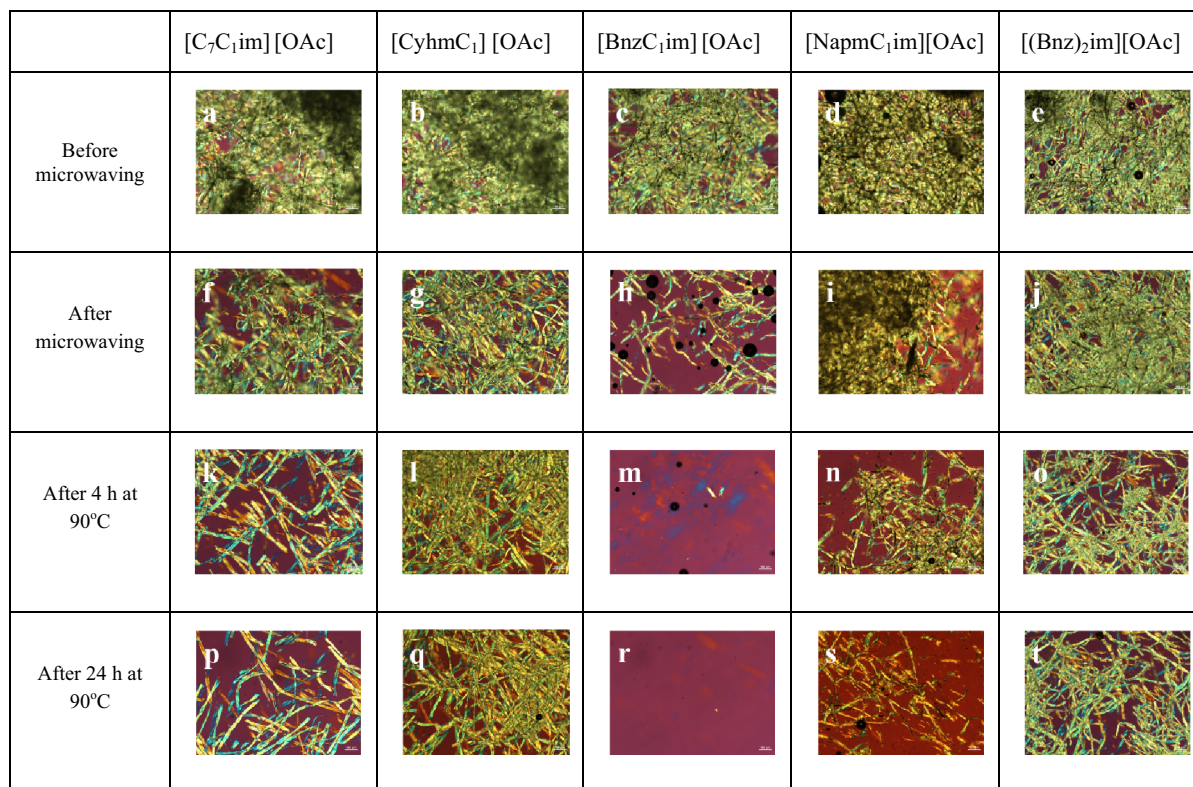


Fig. 1 PLM images of cotton cellulose in ILs at different stages of dissolution. See Table 1 for abbreviations of the ILs

The PLM images show that stirring at 90 °C for 4 h led to complete dissolution in [BnzC₁im][OAc] (Fig. 1m) and varying levels of dissolution in the other four ILs (Fig. 1k, l, n, o). Comparing the images taken after 4 and 24 h at 90 °C to images before microwaving, we find that the degree to which dissolution occurs follows the trend [BnzC₁im][OAc] \gg [NapmC₁im][OAc] > [C₇C₁im][OAc] > [(Bnz)₂im][OAc] > [CyhmC₁im][OAc].

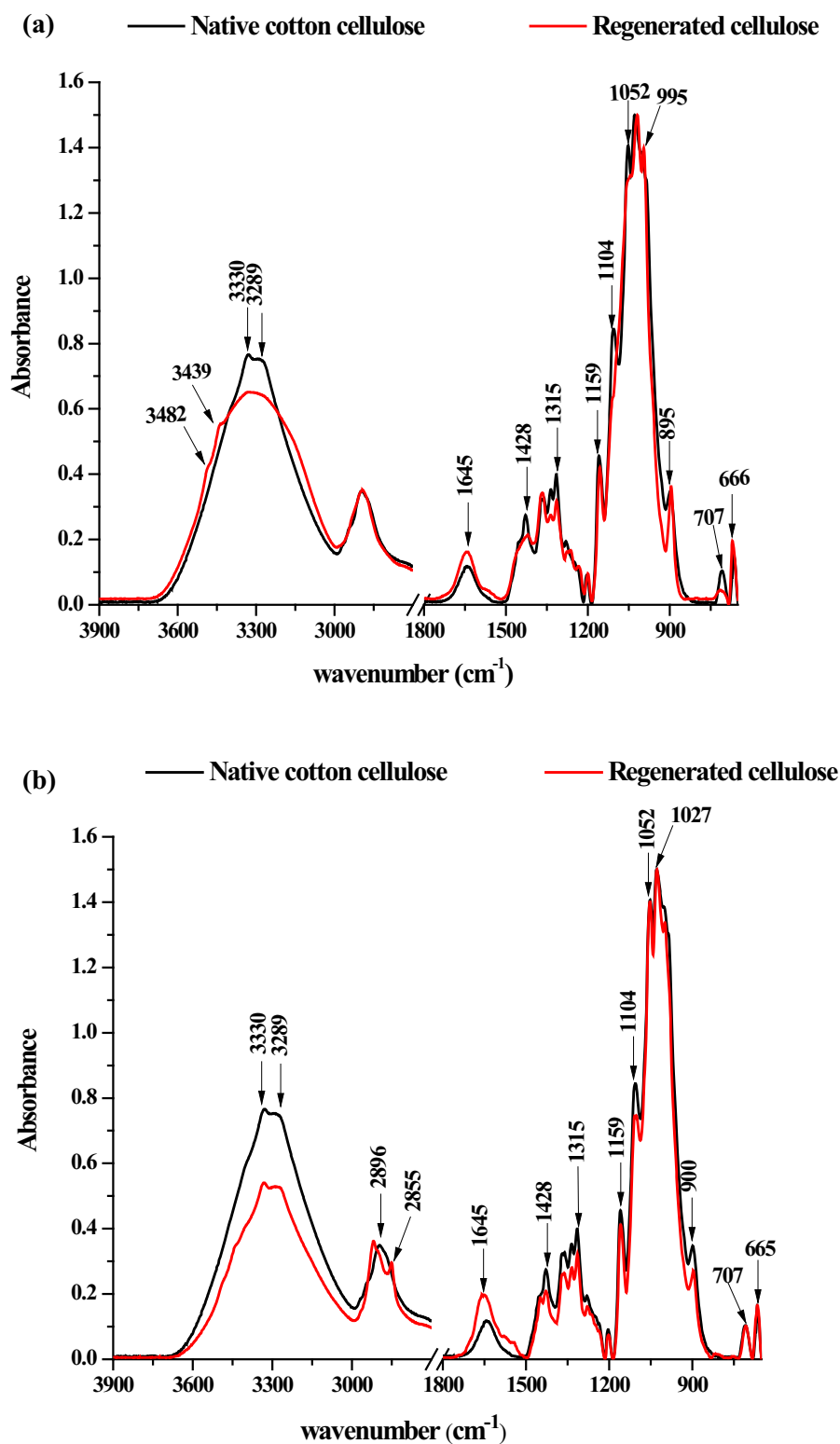
Structure and morphology of regenerated cellulose

FTIR spectra The FTIR spectra of the regenerated cellulose prepared by dissolving cotton in [BnzC₁im][OAc] and [CyhmC₁im][OAc] are shown in Fig. 2a, b respectively (See the Supporting Information for other FTIR spectra of regenerated cellulose from [C₇C₁im][OAc], [NapmC₁im][OAc] and [(Bnz)₂im][OAc]). The FTIR spectrum of native cellulose is quite similar to that of regenerated cellulose in all of the ILs, suggesting that ILs do not affect the chemical structure of cotton cellulose and

regenerated cellulose. However, the FTIR spectrum for regenerated cellulose after dissolution in [BnzC₁im][OAc] exhibits significant changes in the frequencies of the vibrational bands at 3482, 3439, 3330, 3289, 1645, 1428, 1315, 1159, 1104, 1052, 995, 895, 710 and 666 cm⁻¹ compared to frequencies of the corresponding vibrational bands in the spectrum of the starting material. These spectra are consistent with the spectra reported in the literature, indicating that cellulose regenerated from [BnzC₁im][OAc] is in the crystalline form II whereas native cotton cellulose is in the crystalline form I_β (Ilharco et al. 1997; Schwanninger et al. 2004; Oh et al. 2005a, b; Zhang et al. 2005; Abidi et al. 2008, 2014; Salmén and Bergström 2009; Lan et al. 2011; Dassanayake et al. 2016).

The FTIR spectrum of regenerated cellulose after dissolution in [CyhmC₁im][OAc], which was the least effective in dissolving cellulose, showed vibrational bands similar to that of native cotton cellulose (see Fig. 2b). This implies that the regenerated cellulose after dissolution in [CyhmC₁im][OAc] is structurally

Fig. 2 **a** FTIR spectra of ground cotton cellulose and freeze-dried cellulose regenerated after dissolution in [BnzC₁im][OAc]. **b** FTIR spectra of ground cotton cellulose and freeze-dried cellulose regenerated after dissolution in [CyhmC₁m][OAc]



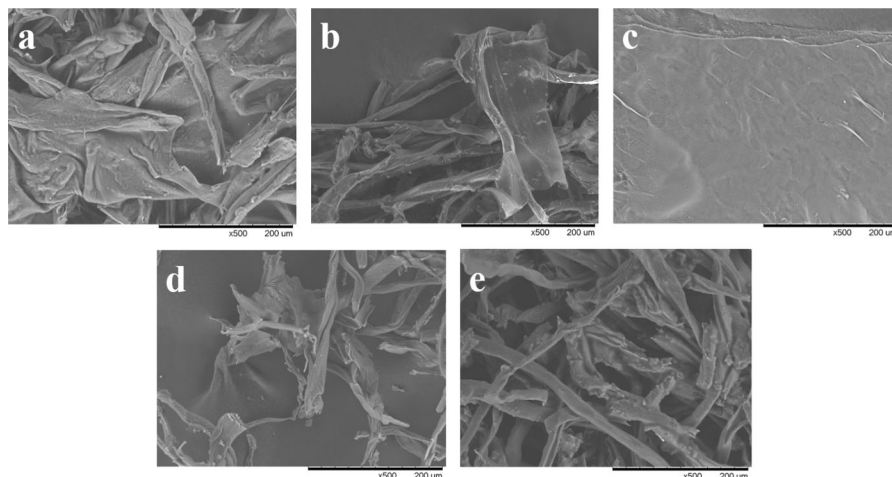


Fig. 3 Scanning electron micrographs of the topography of regenerated cellulose films: **a** [C₇C₁im][OAc]; **b** [CyhmC₁im][OAc]; **c** [BnzC₁im][OAc]; **d** [NapmC₁im][OAc]; **e** [(Bnz)₂im][OAc]

similar to native cotton cellulose and is in the crystalline form I_β. Similar trends were observed in the regenerated cellulose samples after dissolution in the ILs [C₇C₁im][OAc], [NapmC₁im][OAc] and [(Bnz)₂im][OAc] (See Supporting Information). New peaks in the spectra of cellulose regenerated after dissolution in [C₇C₁im][OAc] and [NapmC₁im][OAc] are attributed to the residual IL that remained after rinsing the regenerated cellulose with deionized water (See Supporting Information for the FTIR spectra of neat [C₇C₁im][OAc] and [NapmC₁im][OAc]).

Scanning electron micrographs The surface morphologies of the regenerated films were investigated using scanning electron microscopy. Depicted in Fig. 3a–e are SEM images of regenerated cotton cellulose after dissolution in [C₇C₁im][OAc], [CyhmC₁im][OAc], [BnzC₁im][OAc], [NapmC₁im][OAc] and [(Bnz)₂im][OAc]. Each SEM image was captured under X500 objective magnification. The SEM micrographs in Fig. 3a, b show that the film formed from cellulose regenerated after dissolution in [C₇C₁im][OAc] and [CyhmC₁im][OAc] mainly consists of un-dissolved fibers, indicating incomplete dissolution.

The SEM images show that the structures of the films are characterized by un-dissolved cotton fibers embedded and surrounded by partially dissolved cellulose fibers. In contrast, Fig. 3c shows that cellulose regenerated after dissolution in [BnzC₁im][OAc] forms a uniform film. The absence of un-dissolved

fibers in the film is consistent with the PLM images recorded at 24 h (Fig. 1) that showed complete dissolution of the cotton cellulose. The regenerated films are uniform across the whole surface as indicated by the absence of fractures on the surface. This uniformity is a signature of a dense texture in the cellulose. Similarly, Fig. 3d, e indicate the presence of un-dissolved fibers in the film which is consistent with incomplete dissolution of cotton cellulose in both [NapmC₁im][OAc] and [(Bnz)₂im][OAc]. The SEM images also indicate that the films have homogeneous non-porous structures.

Discussion

The cotton cellulose used in our dissolution experiments has a high degree of polymerization (DP). Most of the reported cellulose dissolution studies in ILs have been performed using microcrystalline cellulose (MCC), which has a significantly lower DP than that of cotton cellulose (Zavrel et al. 2009; Xu et al. 2010). Derecskei and Derecskei-Kovacs used MD simulations to calculate the solubility parameter for series of cellulose oligomers and found that the solubility parameter decreased with increasing MW, which suggests that cellulose with high DP (cotton) is less soluble than cellulose with a lower DP (MCC) (Derecskei and Derecskei-Kovacs 2006). In our study, 5% (w/w) cotton cellulose was completely dissolved in [BnzC₁im][OAc] after 24 h at 90°C, as confirmed by PLM images, which is remarkable considering the

high DP of cotton cellulose. To compare Kosan et al. dissolved 13.2% and 13.5% (w/w) cellulose, respectively, in $[C_4C_1im][OAc]$ and $[C_2C_1][OAc]$ (Kosan et al. 2008). Similarly, Xu et al. dissolved 15% of cellulose in $[C_4C_1im][OAc]$ (Xu et al. 2010). All these studies were performed using MCC. Kosan et al. used light microscopy to monitor the dissolution, whereas Xu et al. used clear solutions as a visual indication of complete dissolution. In contrast to $[BnzC_1im][OAc]$, $[CyhmC_1im][OAc]$ showed a very low capacity to dissolve cellulose. Both cyclohexylmethyl and benzyl have the same number of carbon atoms and are cyclic. The only difference is that the benzyl group is planar and aromatic, whereas the cyclohexylmethyl group is non-planar and non-aromatic. Recent studies by Zavrel et al. and Li et al. showed that introducing unsaturation into the cation (i.e. imidazolium versus pyrrolidinium) increases the transport properties and facilitates the dissolution (Zavrel et al. 2009; Li et al. 2017). In these studies, they only considered the unsaturation of the heterocyclic ring of the cation. An aromatic substituent group, such as benzyl, should affect the dissolution kinetics in a similar way.

The IL $[C_7C_1im][OAc]$ showed poor dissolution of cotton cellulose. This may be attributed to higher viscosity as demonstrated by multiple studies reported in the literature (Zavrel et al. 2009; Zhao et al. 2013; Li et al. 2017). According to these studies, ILs with long alkyl chains have higher viscosity which lowers the mass transport of ions and leads to poor dissolution. Moreover, Zhao et al. demonstrated that cations with short alkyl chains lead to stronger interactions with cellulose than cations with long alkyl chains (Zhao et al. 2012). While mass transport is an important factor in dissolution kinetics, other factors such as size, shape, and conformation of the ions in the IL should also be considered.

ILs with dibenzyl and naphthylmethyl substituent groups showed poor dissolution because of their larger size. Ohno and Fukuya demonstrated that larger cation size leads to higher viscosity, which diminishes the dissolution (Ohno and Fukuya 2009). Meng et al. demonstrated that the cation size affects the cellulose dissolution by using tetraalkylammonium carboxylate ILs. They found that the degree of dissolution strongly depends on the size of the cations (Meng et al. 2017). Further Holding et al. utilized long chain tetraalkylphosphonium ILs, such as

trioctyl(tetradecyl)phosphonium acetate, to dissolve 3% MCC. (Holding et al. 2017).

The effect of viscosity can be mitigated by the addition of cosolvents to the ILs, which increases the fluidity, improves mass transport, and leads to faster dissolution kinetics (Huo et al. 2013; Zhao et al. 2013; Andanson et al. 2014; Velioglu et al. 2014). We performed our dissolution studies at 90 °C in order to achieve faster dissolution. Andanson et al. suggested that from their study with $[C_2C_1im][OAc]$, even though the dissolution process is exothermic, increasing the temperature enhanced the fluidity of the medium, resulting in faster dissolution (Andanson et al. 2015).

There are multiple experimental and theoretical studies aimed at elucidating the mechanism of cellulose dissolution in ILs. Many of these studies were focused on acetate ILs and determining the interaction of acetate with cellulose. In a recent experimental and quantum chemical study, Endo et al. showed that acetate anions at lower concentrations interacted with the hydroxyl groups of cellulose in 1:1 molar ratio, whereas at higher concentrations acetate ions interacted with multiple OH groups of cellulose to form a bridging state (Endo et al. 2016). Further extension of their study found that acetate anions bridge neighboring cellulose chains via OH–O (anion) hydrogen bonds, which facilitates the dissolution (Endo et al. 2017). In MD simulations, Gupta et al. observed significant decrease in the intra- and inter-chain hydrogen bonds when the cellulose fibrils are in contact with acetate anions (Gupta et al. 2011). Ding et al. performed DFT calculations that showed hydrogen bonds in cellulose are weaker than hydrogen bonds formed between ILs and cellulose and that this difference promotes dissolution (Ding et al. 2012). As our focus is on how substituent groups in acetate ILs affect cellulose dissolution, to our knowledge there are only few studies that consider the role of the cation similar to our study.

In an MD simulation study, Schutt et al. confirmed the acetate anion establishes stronger interactions with cellulose and showed that the cation changes the spatial configuration of glucose subunits (Schutt et al. 2016). In a quantum chemistry study of the interactions of ILs with cellobiose by Payal et al. confirmed that both anion and cation are involved in the dissolution (Payal et al. 2012). Gupta et al. demonstrated using MD simulations that the acetate anions

coordinate with cellulose via multiple sites and that the cations form weak hydrophobic interactions with cellulose (Gupta et al. 2011). Another study by Rabideau et al., using model cellulose microfibrils to determine IL-cellulose interactions and mechanisms, confirmed that the anions are tightly bound to cellulose hydroxyl groups and generate a negatively charged complex while cations were in close proximity due to electrostatic attraction (Rabideau et al. 2013).

In our dissolution experiments, the acetate anion can behave in a similar way, as reported in the quantum chemistry calculations and MD simulations, by interacting with cellulose hydroxyl groups via single or multiple sites, thereby disrupting intra- and inter-molecular hydrogen bonds, and generating negatively charged complexes, which initiates the dissolution process. The differences in the dissolution capacity can be rationalized using size, shape, and orientation of the substituents in the cation. Moreover, because of Coulombic attraction, the cation is drawn by the anion into the interior of the cellulose fiber, causing the strands to separate from the main bundle. Clearly, the ability of the cation to intercalate between the strands, causing the strands to separate should be dependent on the size and possibly the shape of the cation. The results of the current study are consistent with this mechanism. For example, cation size is a plausible reason for dissolution being more effective in $[\text{BnzC}_1\text{im}][\text{OAc}]$ than in $[(\text{Bnz})_2\text{im}][\text{OAc}]$. The $[(\text{Bnz})_2\text{im}]^+$ cation with two phenyl groups will have more difficulty intercalating between the strands than the $[\text{BnzC}_1\text{im}]^+$ cation with only one phenyl group. This could be a possible explanation for why $[\text{BnzC}_1\text{im}][\text{OAc}]$ is more effective as a cellulose solvent than $[(\text{Bnz})_2\text{im}][\text{OAc}]$.

The size effect can also be invoked when explaining why cotton cellulose dissolution is more effective in $[\text{BnzC}_1\text{im}][\text{OAc}]$ than in $[\text{NapmC}_1\text{im}][\text{OAc}]$. One could also explain cellulose dissolution being more effective in $[\text{NapmC}_1\text{im}][\text{OAc}]$ than in $[(\text{Bnz})_2\text{im}][\text{OAc}]$ because of a size effect, with the $[\text{NapmC}_1\text{im}]^+$ cation being 11% smaller than $[(\text{Bnz})_2\text{im}]^+$ cation based on the values of van der Waals volume (V_{vdW}) (Table 1). In the case of $[(\text{Bnz})_2\text{im}][\text{OAc}]$, space-filling models show the phenyl groups being in a twisted orientation, which causes the rings to lie in two different planes. In contrast, in the case of $[\text{NapmC}_1\text{im}][\text{OAc}]$, one can think of the planar naphthyl group as being formed by the fusion of two phenyl rings. The

planarity of the naphthyl group allows the cation to slip more easily between the cellulose strands. Thus, factoring the shape effect (twisted versus planar) in addition to the size, one could explain the considerably greater ability for $[\text{NapmC}_1\text{im}][\text{OAc}]$ to dissolve cotton cellulose than $[(\text{Bnz})_2\text{im}][\text{OAc}]$.

In the case of dissolution of cellulose in $[\text{C}_7\text{C}_1\text{im}][\text{OAc}]$ as compared to cellulose dissolution in $[\text{BnzC}_1\text{im}][\text{OAc}]$, the difference can also be attributed to a size effect, given that the $[\text{C}_7\text{C}_1\text{im}]^+$ cation is 17% larger than the $[\text{BnzC}_1\text{im}]^+$ cation. However, $[\text{C}_7\text{C}_1\text{im}][\text{OAc}]$ seems to be an anomaly in that the $[\text{C}_7\text{C}_1\text{im}]^+$ cation being 3% smaller than the $[\text{NapmC}_1\text{im}]^+$ cation one would have predicted cotton cellulose dissolution to be more effective in $[\text{C}_7\text{C}_1\text{im}][\text{OAc}]$ than in $[\text{NapmC}_1\text{im}][\text{OAc}]$, contrary to the actual results. However, the 3% size difference may not be great enough to explain the difference in the abilities of these two ILs to dissolve cellulose. This again suggests that other factors must be playing a role in causing the difference in cellulose dissolution between these two ILs. One possibility is that the heptyl group has more conformational freedom compared to the naphthyl group (18 conformers in the case of $[\text{C}_7\text{C}_1\text{im}]^+$ versus 4 conformers in the case of $[\text{NapmC}_1\text{im}]^+$ as determined by AM1 calculations). This conformational freedom could impede intercalation of the cation between strands in the fiber bundle. In contrast, the naphthyl group being rigid because of its planarity can more easily slide between the strands in the cotton fiber.

Our studies show that of the five ILs, $[\text{CyhmC}_1\text{im}][\text{OAc}]$ is the least effective in dissolving cotton cellulose as evidenced by PLM images that show no fibers in the case of dissolution with $[\text{BnzC}_1\text{im}][\text{OAc}]$ but large amounts of un-dissolved fibers in the case of dissolution with $[\text{CyhmC}_1\text{im}][\text{OAc}]$, even after 24 h (Fig. 11, m). Given that the $[\text{CyhmC}_1\text{im}]^+$ cation is only 4% larger than the $[\text{BnzC}_1\text{im}]^+$ cation, based on the values of V_{vdW} (Table 1), the difference in the ability of these two ILs to dissolve cellulose cannot be due just to a size effect. The difference could be due to a shape effect in that the planarity of the phenyl groups in the $[\text{BnzC}_1\text{im}]^+$ and $[(\text{Bnz})_2\text{im}]^+$ cations and the planarity of the naphthyl group in the $[\text{NapmC}_1\text{im}]^+$ cation helps these cations to intercalate between cellulose strands of the cotton, thus promoting peeling of strands from the fiber. In contrast, the bulkiness and larger size of the cyclohexyl group compared to the

phenyl group introduces steric effects on the cation that minimize the penetration of the cation between the strands of cellulose. Unlike the phenyl group, the cyclohexyl group is not planar due to the fact that it can either be in the boat or chair configuration. The differences in kinetics can be attributed to differences in the fluidities of these ILs. The ILs with higher fluidity, faster dissolution kinetics. The recent review by Li et al. summarizes mechanistic studies of cellulose dissolution in ILs and discusses the synergistic mechanism in detail. There are still many contradicting results, and more studies are required to ascertain the mechanism (Li et al. 2018).

Conclusions

This study provides a plausible molecular-level explanation for the role of the cation in the dissolution of cotton cellulose in ILs. [CyhmC₁im][OAc] and [(Bnz)₂im][OAc] performed poorly in the dissolution of cotton cellulose due to the larger size of the cations. Although we have not measured the viscosities of these ILs, the larger size of [(Bnz)₂im]⁺ compared to [BnzC₁im]⁺ should result in a higher viscosity, which contributes to poor cellulose dissolution. On the other hand, [BnzC₁im][OAc] showed a significant capacity to dissolve cotton cellulose due to the unsaturated nature and the planarity of the benzyl group and was the most effective of the five ILs in this study. The poor dissolution capacity of [C₇C₁im][OAc] is mainly attributed to long alkyl chain which leads to an increase in the viscosity and lower mass transport of ions. Increasing the size of the cation has an adverse effect on cotton cellulose dissolution (e.g., [BnzC₁im][OAc] versus [(Bnz)₂im][OAc]). We also confirm that the shape of the cation plays a role in that the bulkiness of the cation (e.g., [CyhmC₁im][OAc]) has an adverse effect on cotton cellulose dissolution, whereas the planarity of the cation (e.g., [BnzC₁im][OAc]) seems to have a positive effect on cotton cellulose dissolution. The fact that the benzyl substituent is unsaturated, whereas the cyclohexylmethyl group is saturated may also explain why [BnzC₁im][OAc] is better in dissolving cellulose compared to [CyhmC₁im][OAc]. In the case of [NapmC₁im][OAc] versus [(Bnz)₂im][OAc], [(Bnz)₂im][OAc] is less effective in dissolving cotton cellulose than [NapmC₁im][OAc], not only because the [(Bnz)₂im]⁺ cation is 11% larger

in size than [NapmC₁im]⁺ cation, but because of the twisted configuration of the phenyl groups in [(Bnz)₂im]⁺ as opposed to the planarity of the naphthyl group in [NapmC₁im]⁺. Apart from size, shape, and bulkiness of these ILs, the viscosity plays a role in determining the ability of these ILs to dissolve cellulose. Further work in our labs is aimed at measuring the viscosities of these ILs.

Acknowledgments The authors thank Bayer Crop Science for their financial support. The authors would like to knowledge Yu Zhang for her assistance in ionic liquid synthesis.

References

- Abe M, Fukaya Y, Ohno H (2010) Extraction of polysaccharides from bran with phosphonate or phosphinate-derived ionic liquids under short mixing time and low temperature. *Green Chem* 12:1274. <https://doi.org/10.1039/c003976d>
- Abidi N, Hequet E, Cabrales L et al (2008) Evaluating cell wall structure and composition of developing cotton fibers using fourier transform infrared spectroscopy and thermogravimetric analysis. *J Appl Polym Sci* 107:476–486. <https://doi.org/10.1002/app.27100>
- Abidi N, Cabrales L, Haigler CH (2014) Changes in the cell wall and cellulose content of developing cotton fibers investigated by FTIR spectroscopy. *Carbohydr Polym* 100:9–16. <https://doi.org/10.1016/j.carbpol.2013.01.074>
- Andanson J-M, Bordes E, Devémy J et al (2014) Understanding the role of co-solvents in the dissolution of cellulose in ionic liquids. *Green Chem* 16:2528. <https://doi.org/10.1039/c3gc42244e>
- Andanson JM, Pádua AAH, Costa Gomes MF (2015) Thermodynamics of cellulose dissolution in an imidazolium acetate ionic liquid. *Chem Commun* 51:4485–4487. <https://doi.org/10.1039/c4cc10249e>
- Azizi Samir MAS, Alloin F, Dufresne A (2005) Review of recent research into cellulosic whiskers, their properties and their application in nanocomposite field. *Biomacromol* 6:612–626
- Casas A, Palomar J, Alonso MV et al (2012) Comparison of lignin and cellulose solubilities in ionic liquids by COSMO-RS analysis and experimental validation. *Ind Crops Prod* 37:155–163. <https://doi.org/10.1016/j.indcrop.2011.11.032>
- Casas A, Omar S, Palomar J et al (2013) Relation between differential solubility of cellulose and lignin in ionic liquids and activity coefficients. *RSC Adv* 3:3453–3460. <https://doi.org/10.1039/c2ra22800a>
- Dassanayake RS, Gunathilake C, Jackson T et al (2016) Preparation and adsorption properties of aerocellulose-derived activated carbon monoliths. *Cellulose* 23:1363–1374. <https://doi.org/10.1007/s10570-016-0886-1>
- Derecskei B, Derecskei-Kovacs A (2006) Molecular dynamic studies of the compatibility of some cellulose derivatives with selected ionic liquids. *Mol Simul* 32:109–115. <https://doi.org/10.1080/08927020600669627>

- Ding ZD, Chi Z, Gu WX et al (2012) Theoretical and experimental investigation on dissolution and regeneration of cellulose in ionic liquid. *Carbohydr Polym* 89:7–16. <https://doi.org/10.1016/j.carbpol.2012.01.080>
- Endo T, Hosomi S, Fujii S et al (2016) Anion bridging-induced structural transformation of cellulose dissolved in ionic liquid. *J Phys Chem Lett* 7:5156–5161. <https://doi.org/10.1021/acs.jpcclett.6b02504>
- Endo T, Hosomi S, Fujii S et al (2017) Nano-structural investigation on cellulose highly dissolved in ionic liquid: a small angle x-ray scattering study. *Molecules*. <https://doi.org/10.3390/molecules22010178>
- Gericke M, Fardim P, Heinze T (2012) Ionic liquids—promising but challenging solvents for homogeneous derivatization of cellulose. *Molecules* 17:7458–7502
- Gupta KM, Jiang J (2015) Cellulose dissolution and regeneration in ionic liquids: a computational perspective. *Chem Eng Sci* 121:180–189. <https://doi.org/10.1016/j.ces.2014.07.025>
- Gupta KM, Hu Z, Jiang J (2011) Mechanistic understanding of interactions between cellulose and ionic liquids: a molecular simulation study. *Polymer (Guildf)* 52:5904–5911. <https://doi.org/10.1016/j.polymer.2011.10.035>
- Haigler CH, Betancur L, Stiff MR, Tuttle JR (2012) Cotton fiber: a powerful single-cell model for cell wall and cellulose research. *Front Plant Sci*. <https://doi.org/10.3389/fpls.2012.00104>
- Heinze T, Dorn S, Schöbitz M et al (2008) Interactions of ionic liquids with polysaccharides—2: Cellulose. In: *Macromolecular Symposia*, pp 8–22
- Holding AJ, Parviainen A, Kilpeläinen I et al (2017) Efficiency of hydrophobic phosphonium ionic liquids and DMSO as recyclable cellulose dissolution and regeneration media. *RSC Adv* 7:17451–17461. <https://doi.org/10.1039/c7ra01662j>
- Huo F, Liu Z, Wang W (2013) Cosolvent or antisolvent? A molecular view of the interface between ionic liquids and cellulose upon addition of another molecular solvent. *J Phys Chem B* 117:11780–11792. <https://doi.org/10.1021/jp407480b>
- Ilharco LM, Garcia AR, Lopes da Silva J, Vieira Ferreira LF (1997) Infrared approach to the study of adsorption on cellulose: influence of cellulose crystallinity on the adsorption of benzophenone. *Langmuir* 13:4126–4132. <https://doi.org/10.1021/la962138u>
- Kahlen J, Masuch K, Leonhard K (2010) Modelling cellulose solubilities in ionic liquids using COSMO-RS. *Green Chem* 12:2172–2181. <https://doi.org/10.1039/c0gc00200c>
- Kosan B, Michels C, Meister F (2008) Dissolution and forming of cellulose with ionic liquids. *Cellulose* 15:59–66. <https://doi.org/10.1007/s10570-007-9160-x>
- Lan W, Liu CF, Yue FX et al (2011) Ultrasound-assisted dissolution of cellulose in ionic liquid. *Carbohydr Polym* 86:672–677. <https://doi.org/10.1016/j.carbpol.2011.05.013>
- Li Y, Liu X, Zhang S et al (2015) Dissolving process of a cellulose bunch in ionic liquids: a molecular dynamics study. *Phys Chem Chem Phys* 17:17894–17905. <https://doi.org/10.1039/C5CP02009C>
- Li Y, Liu X, Zhang Y et al (2017) Why only ionic liquids with unsaturated heterocyclic cations can dissolve cellulose: a simulation study. *ACS Sustain Chem Eng* 5:3417–3428. <https://doi.org/10.1021/acssuschemeng.7b00073>
- Li Y, Wang J, Liu X, Zhang S (2018) Towards a molecular understanding of cellulose dissolution in ionic liquids: anion/cation effect, synergistic mechanism and physico-chemical aspects. *Chem Sci* 9:4027–4043
- Lindman B, Karlström G, Stigsson L (2010) On the mechanism of dissolution of cellulose. *J Mol Liq* 156:76–81. <https://doi.org/10.1016/j.molliq.2010.04.016>
- Liu H, Sale KL, Holmes BM et al (2010) Understanding the interactions of cellulose with ionic liquids: a molecular dynamics study. *J Phys Chem B* 114:4293–4301. <https://doi.org/10.1021/jp9117437>
- Liu Y-R, Thomsen K, Nie Y et al (2016) Predictive screening of ionic liquids for dissolving cellulose and experimental verification. *Green Chem* 18:6246–6254. <https://doi.org/10.1039/C6GC01827K>
- Lu B, Xu A, Wang J (2014) Cation does matter: how cationic structure affects the dissolution of cellulose in ionic liquids. *Green Chem* 16:1326–1335. <https://doi.org/10.1039/C3GC41733F>
- Madeira Lau R, Sorgesdrager MJ, Carrea G et al (2004) Dissolution of *Candida antarctica* lipase B in ionic liquids: effects on structure and activity. *Green Chem* 6:483–487. <https://doi.org/10.1039/B405693K>
- Meng X, Devemy J, Verney V et al (2017) Improving cellulose dissolution in ionic liquids by tuning the size of the ions: impact of the length of the alkyl chains in tetraalkylammonium carboxylate. *Chemsuschem* 10:1749–1760. <https://doi.org/10.1002/cssc.201601830>
- Mostofian B, Smith JC, Cheng X (2011) The solvation structures of cellulose microfibrils in ionic liquids. *Interdiscip Sci Comput Life Sci* 3:308–320. <https://doi.org/10.1007/s12539-011-0111-8>
- Mostofian B, Cheng X, Smith JC (2014) Replica-exchange molecular dynamics simulations of cellulose solvated in water and in the ionic liquid 1-butyl-3-methylimidazolium chloride. *J Phys Chem B* 118:11037–11049. <https://doi.org/10.1021/jp502889c>
- Oh SY, Il Yoo D, Shin Y et al (2005a) Crystalline structure analysis of cellulose treated with sodium hydroxide and carbon dioxide by means of X-ray diffraction and FTIR spectroscopy. *Carbohydr Res* 340:2376–2391. <https://doi.org/10.1016/j.carres.2005.08.007>
- Oh SY, Il Yoo D, Shin Y, Seo G (2005b) FTIR analysis of cellulose treated with sodium hydroxide and carbon dioxide. *Carbohydr Res* 340:417–428. <https://doi.org/10.1016/j.carres.2004.11.027>
- Ohno H, Fukaya Y (2009) Task specific ionic liquids for cellulose technology. *Chem Lett* 38:2–7. <https://doi.org/10.1246/cl.2009.2>
- Olsson C, Westman G (2013) Direct dissolution of cellulose: background, means and applications. *Cellul Asp*. <https://doi.org/10.5772/52144>
- Payal RS, Bharath R, Periyasamy G, Balasubramanian S (2012) Density functional theory investigations on the structure and dissolution mechanisms for cellobiose and xylan in an ionic liquid: gas phase and cluster calculations. *J Phys Chem B* 116:833–840. <https://doi.org/10.1021/jp207989w>
- Phillips DM, Drummy LF, Conrady DG et al (2004) Dissolution and regeneration of *Bombyx mori* silk fibroin using ionic

- liquids. *J Am Chem Soc* 126:14350–14351. <https://doi.org/10.1021/ja046079f>
- Pinkert A, Marsh KN, Pang S, Staiger MP (2009) Ionic liquids and their interaction with cellulose. *Chem Rev* 109:6712–6728. <https://doi.org/10.1021/cr9001947>
- Rabideau BD, Agarwal A, Ismail AE (2013) Observed mechanism for the breakup of small bundles of cellulose I α and I β in ionic liquids from molecular dynamics simulations. *J Phys Chem B* 117:3469–3479. <https://doi.org/10.1021/jp310225t>
- Rabideau BD, Agarwal A, Ismail AE (2014) The role of the cation in the solvation of cellulose by imidazolium-based ionic liquids. *J Phys Chem B* 118:1621–1629. <https://doi.org/10.1021/jp4115755>
- Ragauskas AJ, Williams CK, Davison BH et al (2006) The path forward for biofuels and biomaterials. *Science* 311:484–489
- Remsing RC, Swatoski RP, Rogers RD, Moyna G (2006) Mechanism of cellulose dissolution in the ionic liquid 1-n-butyl-3-methylimidazolium chloride: a ¹³C and ^{35/37}Cl NMR relaxation study on model systems. *Chem Commun*. <https://doi.org/10.1039/b600586c>
- Remsing RC, Hernandez G, Swatoski RP et al (2008) Solvation of carbohydrates in *N,N'*-dialkylimidazolium ionic liquids: a multinuclear NMR spectroscopy study. *J Phys Chem B* 112:11071–11078. <https://doi.org/10.1021/jp8042895>
- Rogers RD, Seddon KR (2003) Ionic liquids—solvents of the future? *Science* 302:792–793
- Salmén L, Bergström E (2009) Cellulose structural arrangement in relation to spectral changes in tensile loading FTIR. *Cellulose* 16:975–982. <https://doi.org/10.1007/s10570-009-9331-z>
- Schutt TC, Bharadwaj VS, Hegde GA et al (2016) In silico insights into the solvation characteristics of the ionic liquid 1-methyltriethoxy-3-ethylimidazolium acetate for cellulosic biomass. *Phys Chem Chem Phys* 18:23715–23726. <https://doi.org/10.1039/c6cp03235d>
- Schwanner M, Rodrigues JC, Pereira H, Hinterstoisser B (2004) Effects of short-time vibratory ball milling on the shape of FT-IR spectra of wood and cellulose. *Vib Spectrosc* 36:23–40. <https://doi.org/10.1016/j.vibspec.2004.02.003>
- Sun N, Rodríguez H, Rahman M, Rogers RD (2011) Where are ionic liquid strategies most suited in the pursuit of chemicals and energy from lignocellulosic biomass? *Chem Commun* 47:1405–1421. <https://doi.org/10.1039/C0CC03990J>
- Swatoski RP, Spear SK, Holbrey JD, Rogers RD (2002) Dissolution of cellose with ionic liquids. *J Am Chem Soc* 124:4974–4975. <https://doi.org/10.1021/ja025790m>
- Thakurathi M, Gurung E, Cetin MM et al (2018) The Stokes-Einstein equation and the diffusion of ferrocene in imidazolium-based ionic liquids studied by cyclic voltammetry: effects of cation ion symmetry and alkyl chain length. *Electrochim Acta*. <https://doi.org/10.1016/j.electacta.2017.10.149>
- Velioglu S, Yao X, Devémy J et al (2014) Solvation of a cellulose microfibril in imidazolium acetate ionic liquids: effect of a cosolvent. *J Phys Chem B* 118:14860–14869. <https://doi.org/10.1021/jp508113a>
- Vitz J, Erdmenger T, Haensch C, Schubert US (2009) Extended dissolution studies of cellulose in imidazolium based ionic liquids. *Green Chem* 11:417–424. <https://doi.org/10.1039/b818061j>
- Welton T (1999) Room-temperature ionic liquids. Solvents for synthesis and catalysis. *Chem Rev* 99:2071–2084. <https://doi.org/10.1021/cr980032t>
- Xu A, Wang J, Wang H (2010) Effects of anionic structure and lithium salts addition on the dissolution of cellulose in 1-butyl-3-methylimidazolium-based ionic liquid solvent systems. *Green Chem* 12:268–275. <https://doi.org/10.1039/B916882F>
- Xu H, Pan W, Wang R et al (2012) Understanding the mechanism of cellulose dissolution in 1-butyl-3-methylimidazolium chloride ionic liquid via quantum chemistry calculations and molecular dynamics simulations. *J Comput Aided Mol Des* 26:329–337. <https://doi.org/10.1007/s10822-012-9559-9>
- Yao Y, Li Y, Liu X et al (2015) Mechanistic study on the cellulose dissolution in ionic liquids by density functional theory. *Chin J Chem Eng* 23:1894–1906. <https://doi.org/10.1016/j.cjche.2015.07.018>
- Youngs TGA, Holbrey JD, Deetlefs M et al (2006) A molecular dynamics study of glucose solvation in the ionic liquid 1,3-dimethylimidazolium chloride. *ChemPhysChem* 7:2279–2281. <https://doi.org/10.1002/cphc.200600569>
- Youngs TGA, Hardacre C, Holbrey JD (2007) Glucose solvation by the ionic liquid 1,3-dimethylimidazolium chloride: a simulation study. *J Phys Chem B* 111:13765–13774. <https://doi.org/10.1021/jp076728k>
- Youngs TGA, Holbrey JD, Mullan CL et al (2011) Neutron diffraction, NMR and molecular dynamics study of glucose dissolved in the ionic liquid 1-ethyl-3-methylimidazolium acetate. *Chem Sci* 2:1594. <https://doi.org/10.1039/c1sc00241d>
- Zavrel M, Bross D, Funke M et al (2009) High-throughput screening for ionic liquids dissolving (ligno-)cellulose. *Bioresour Technol* 100:2580–2587. <https://doi.org/10.1016/j.biortech.2008.11.052>
- Zhang H, Wu J, Zhang J, He J (2005) 1-allyl-3-methylimidazolium chloride room temperature ionic liquid: a new and powerful nonderivatizing solvent for cellulose. *Macromolecules* 38:8272–8277. <https://doi.org/10.1021/ma0505676>
- Zhang S, Sun N, He X et al (2006) Physical properties of ionic liquids: database and evaluation. *J Phys Chem Ref Data* 35:1475–1517
- Zhao H, Baker GA, Song Z et al (2008) Designing enzyme-compatible ionic liquids that can dissolve carbohydrates. *Green Chem* 10:696–705. <https://doi.org/10.1039/b801489b>
- Zhao D, Li H, Zhang J et al (2012) Dissolution of cellulose in phosphate-based ionic liquids. *Carbohydr Polym* 87:1490–1494. <https://doi.org/10.1016/j.carbpol.2011.09.045>
- Zhao Y, Liu X, Wang J, Zhang S (2013) Insight into the cosolvent effect of cellulose dissolution in imidazolium-based ionic liquid systems. *J Phys Chem B* 117:9042–9049. <https://doi.org/10.1021/jp4038039>